

Grigoris Maravelias^{1,2}, Stephan de Wit^{1,3}, Alceste Bonanos¹, Frank Tramper⁴, Gonzalo Munoz-Sanchez^{1,3}, Evangelia Christodoulou^{1,3}

(1) National Observatory of Athens, Greece, (2) FORTH, Greece, (3) National & Kapodistrian Univ. of Athens, Greece, (4) KU Leuven, Belgium

Table 1. Properties of galaxies examined in this work.

ID	R.A. (J2000)	Dec. (J2000)	Gal. Type	Distance (Mpc)	Metal. ¹ (Z _⊙)	RV ^{1,2} (km s ⁻¹)
(1)	(2)	(3)	(4)	(5)	(6)	(7)
WLM	00:01:58	-15:27:39	SB(s)m: sp	0.98±0.04	0.14	-130±1
NGC 55	00:14:53	-39:11:48	SB(s)m: sp	1.87±0.02	0.27	129±2
IC 10	00:20:17	+59:18:14	dIrr IV/BCD	0.80±0.03	0.45	-348±1
NGC 247	00:47:09	-20:45:37	SAB(s)d	3.03±0.03	0.40	156
NGC 253	00:47:33	-25:17:18	SAB(s)c	3.40±0.06	0.72	259
NGC 300	00:54:53	-37:41:04	SA(s)d	1.97±0.06	0.41	146±2
NGC 1313	03:18:16	-66:29:54	SB(s)d	4.61±0.17	0.57	470
NGC 3109	10:03:07	-26:09:35	SB(s)m edge-on	1.27±0.03	0.21	403±2
Sextans A	10:11:01	-04:41:34	IBm	1.34±0.02	0.06	324±2
M83	13:37:01	-29:51:56	SAB(s)c	4.90±0.20	1.58	519
NGC 6822	19:44:58	+14:48:12	IB(s)m	0.45±0.01	0.32	-57±2
NGC 7793	23:57:50	-32:35:28	SA(s)d	3.47±0.04	0.42	227

¹ The numbers presented here reflect the mean value per galaxy.

² The RV errors correspond to the statistical error and not the systemic one which is (typically) larger.

Table 2. Properties of the sources identified in this work, along with the RV values and the spectral classification as derived from this work, and that from literature (for those sources that is available).

Name	RA (J2000)	Dec (J2000)	Prio.	ID ¹	SNR ²	SpT	Prev. SpT	RV (km s ⁻¹)
(1)	(2)	(3)	(4)	(5)	(6)	(7)	(8)	(9)
WLM-1	00:02:02.32	-15:27:43.81	Y	95	30	B[e]SG	Fe star	-48±10
NGC55-1	00:15:09.31	-39:12:41.62	Y	178	18	B[e]SG	-	156±31
NGC55-2	00:15:18.54	-39:13:12.32	N	736	46	LBVc	LBVc/WN11	105±38
NGC55-3	00:15:37.66	-39:13:48.68	N	2924	50	LBVc	LBVc/WN11	202±30
NGC247-1	00:47:02.17	-20:47:40.13	Y	246	26	B[e]SG	B[e]SG	217±12
NGC247-2	00:47:03.91	-20:43:17.22	N	1192	44	LBVc	-	114±41
NGC253-1	00:47:04.90	-25:20:44.12	Y	739	3	B[e]SG	-	283±56
NGC300-1	00:55:27.93	-37:44:19.61	Y	67	44	B[e]SG	-	58±27
NGC300-2	00:55:19.17	-37:40:56.53	Y	389	9	B[e]SG	-	121±34
NGC3109-1	10:03:02.11	-26:08:58.06	Y	188	70	LBVc	-	371±29
NGC7793-1	23:57:43.28	-32:34:01.81	N	111	19	B[e]SG c	-	317±32

¹ This ID corresponds to the *Spitzer* source numbering as used throughout the ASSESS project (see Tramper et al., in prep., and Munoz-Sanchez et al., in prep., for the use with full catalogs).

² Estimated by averaging the SNR over the ranges 6000–6150Å and 6950–7100Å.

Abstract

Mass loss is one of the key parameters that determine stellar evolution. Despite the progress we have achieved over the last decades we still cannot match the observational derived values with theoretical predictions. Even worse, there are certain phases, such as the B[e] supergiants (B[e]SGs) and the Luminous Blue Variables (LBVs), where significant mass is lost through episodic or outburst activity. This leads to various structures around them that permit dust formation, making these objects bright IR sources. The ASSESS project aims to determine the role of episodic mass, by examining large numbers of cool and hot objects (such as B[e]SGs/LBVs). For this, we initiated a large observing campaign to obtain spectroscopic data for ~1000 IR selected sources in 27 nearby galaxies. Within this project we successfully identified 6 B[e] supergiants and 5 Luminous Blue Variables of which 5 and 3, respectively, are new discoveries. We used spectroscopic, photometric and light curve information to better constrain the nature of the reported objects. We particularly note the presence of B[e]SGs at metallicity environments as low as 0.14Z_⊙.

Target Selection and Observations

Source catalogs were created by first matching *Spitzer* point-source catalogs with Pan-STARRS data (*Gaia* was used for foreground cleaning), and then by screening sources to minimize the contamination by AGB stars (absolute magnitude cut of $M_{[3.6]}\leq-9.0$ mag) and background IR galaxies/quasars (cut at $m_{[4.5]}\leq 15.5$ mag; see Tramper et al., in prep.). To select best candidates (dusty sources) we applied a color term cut $m_{[3.6]} - m_{[4.5]} > 0.1$ mag. Depending on the galaxy size we ended up with a few tens to hundreds of targets per galaxy. To obtain spectroscopic data we required instruments with multi-object spectroscopic modes; OSIRIS/GTC (R~600, 5300-9800Å), and FORS2/ESO (R~1000, 5200-8700Å). During the campaign we were able to robustly classify (after careful visual inspection) 465 objects in the 12 targeted galaxies (Table 1). Only 11 out of all these (~3%) contain features in their optical spectra that indicate a B[e]SG/LBV nature (other sources being RSGs (~37%), other Blue/Yellow Supergiants (~7/5%), emission objects (~2%), carbon stars (~6%), AGN/QSO/background galaxies (~4%), HII regions (~22%), foreground sources (~14%). In Table 2 we present the identified objects.

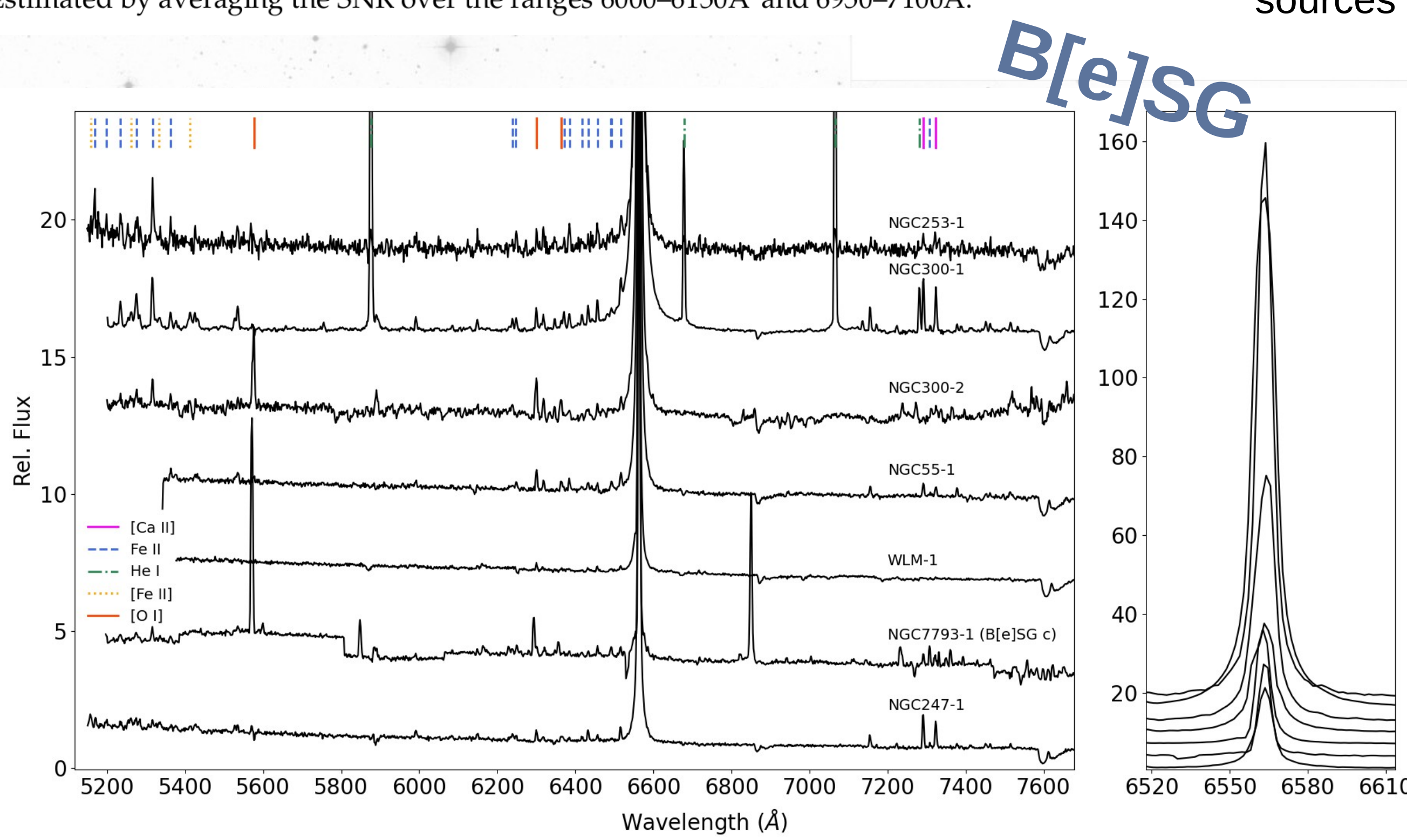
Galaxies 2023, vol. 11, 79



maravelias@noa.gr

Null Detections

We note that although the same approach was followed for all 12 galaxies, we got null results for five of them: IC 10, NGC 1313, Sextans A, M83, NGC 6822. The contamination of HII regions is increased for galaxies further away (NGC 1313, M83), while other reasons (sources failing to pass the selection criteria, technical issues such as target positioning in the masks, detector gaps, etc) resulted into no detections.



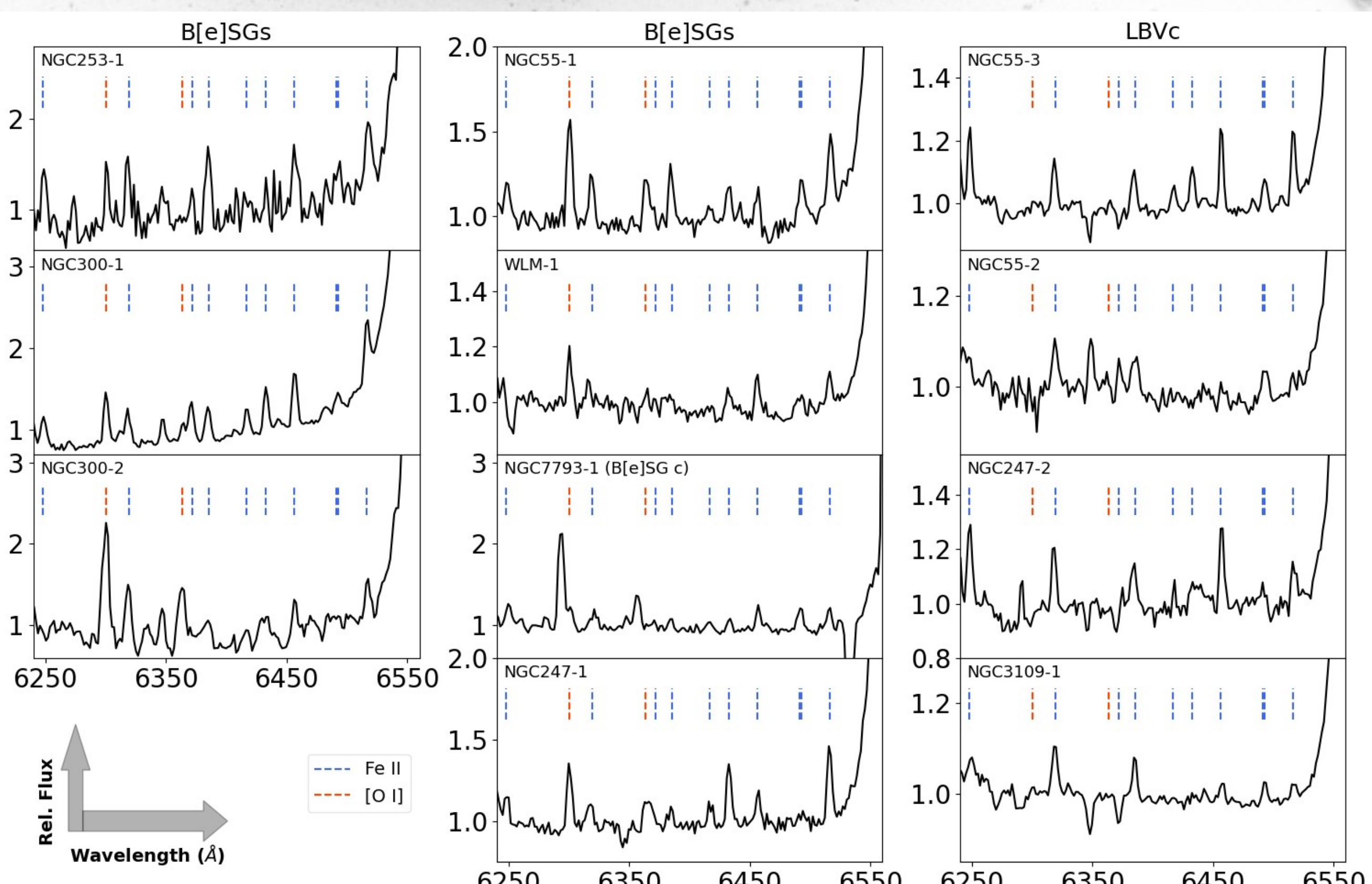
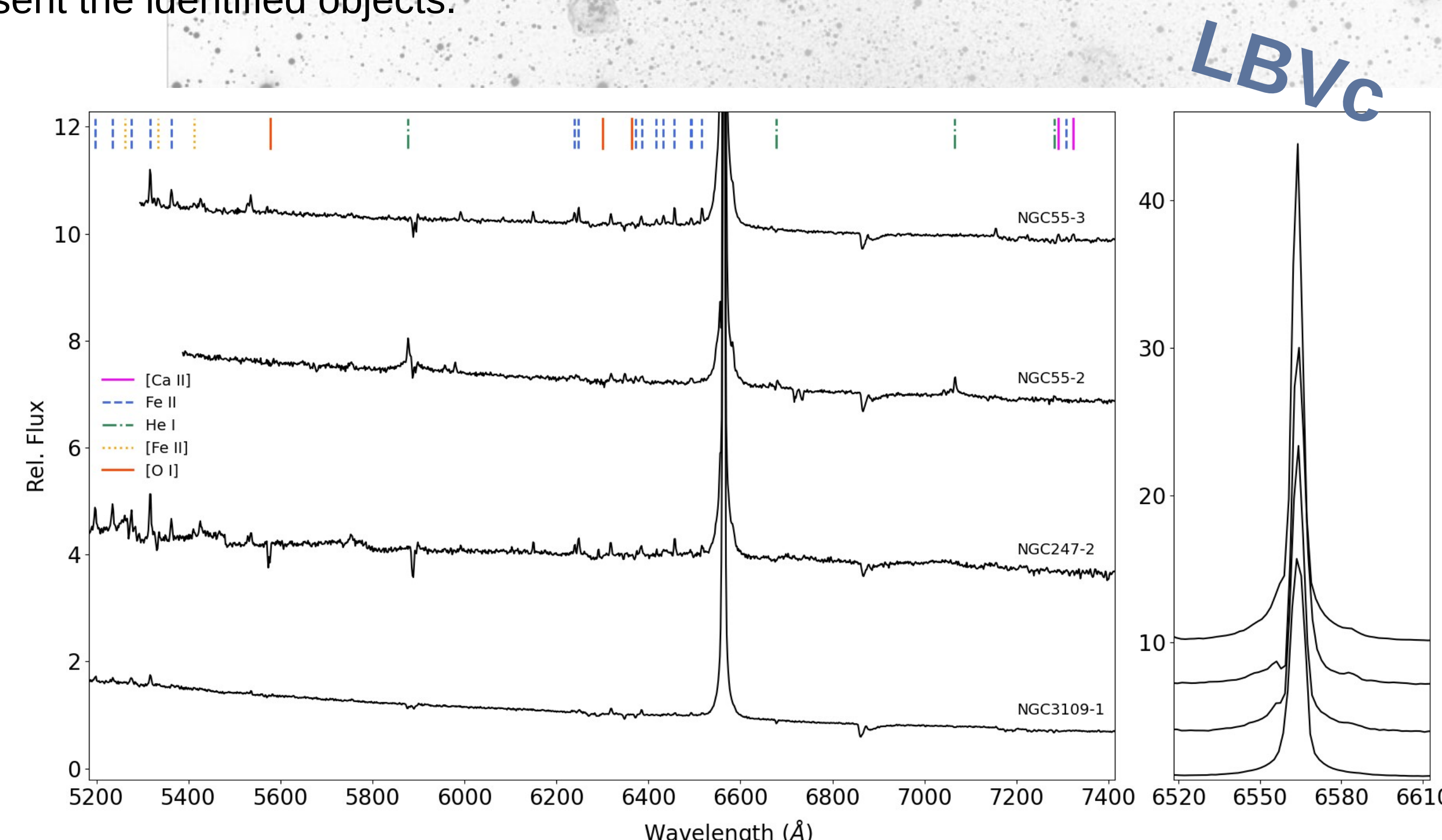
Classification

Both B[e]SG and LBVc can display:

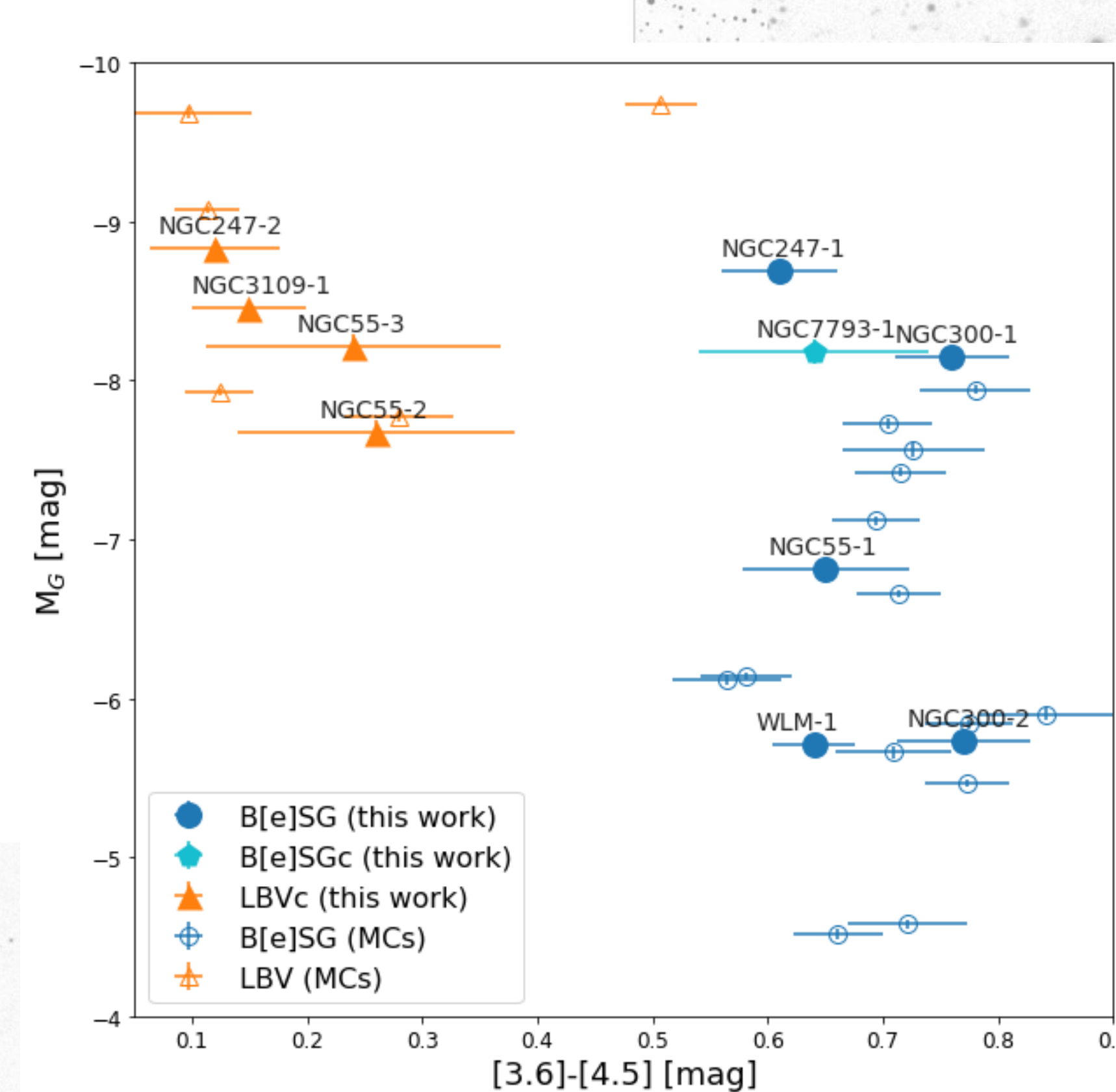
- Strong H α emission
- Fe lines in emission
- [Fe] and [Ca II] lines

but ONLY B[e]SG present [O I] λ 6300.

Without any information on spectral and photometric variability these targets are LBVc candidates.



The region bluewards of H α . The [O I] λ 6300 line is characteristic of B[e]SGs [1,2]. The presence of [Fe] is more evident in B[e]SG while LBVs may or may not display them [3]. The Fe lines in this region were used to estimate the radial velocity of all sources (Table 2) which, within the error margins, are compatible with those of their host galaxies (Table 1). NGC7793-1 suffers from various artifacts and a clear classification from the spectrum alone is not possible (see the CMD plot).

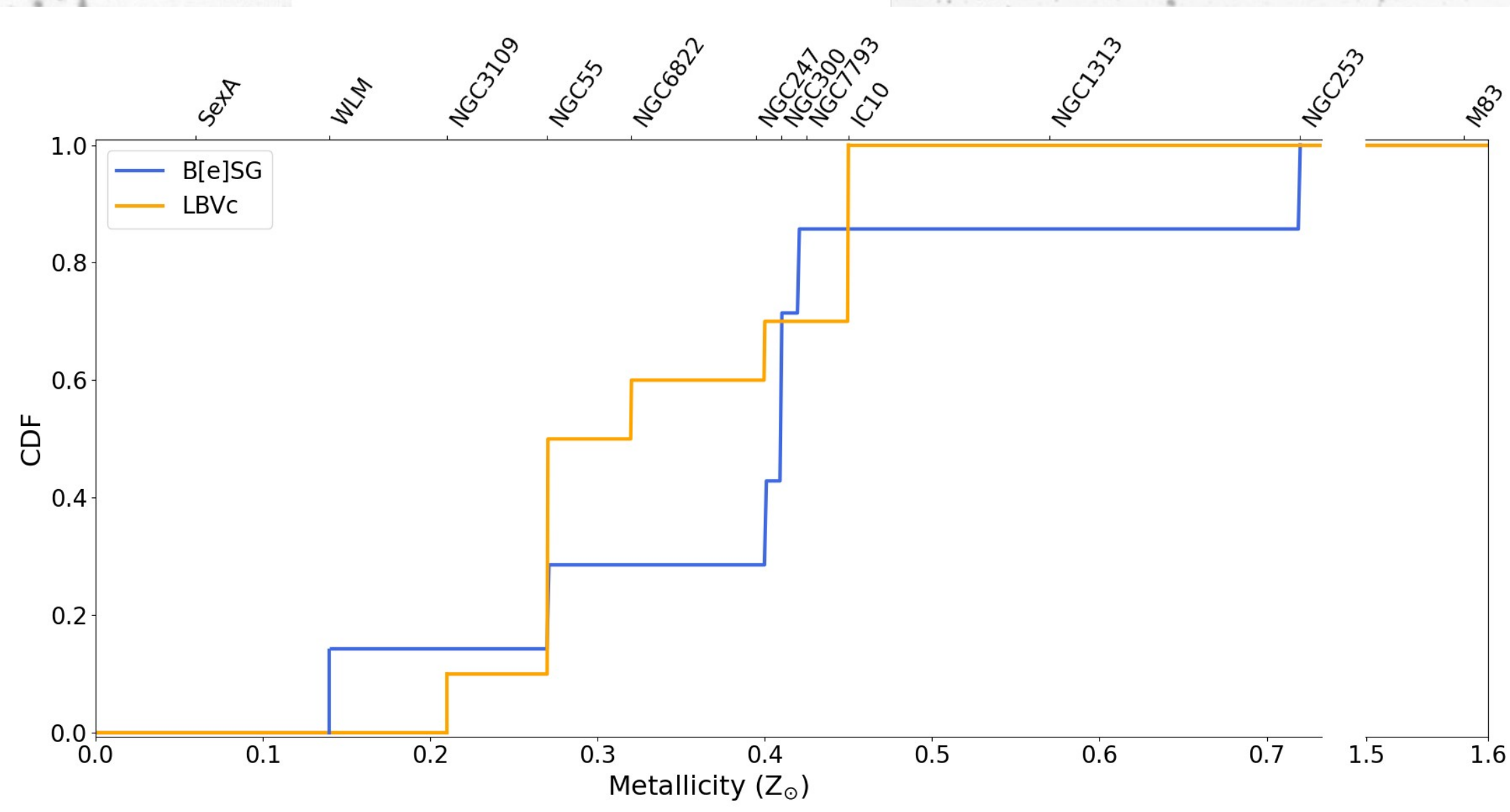


Separating the two classes

CMD plot of *Spitzer* [3.6]-[4.5] vs. absolute optical M_G (*Gaia*) magnitude. We include all our sample as well as the Magellanic Cloud sources from [4]. There is a clear separation between the two classes. The presence of hotter dusty environments becomes more significant for B[e]SGs, as they look redder than LBVs, which they populate the upper left part of the plot. Therefore, very bright optical sources with IR color up to ~0.5 mag are most probably LBVs, while sources with color > 0.5 mag would be B[e]SG (at almost any G magnitude). We highlight the position of NGC7793-1, which is located among the B[e]SGs of our sample and of the Magellanic Clouds. Therefore, we consider it as a candidate B[e]SG.

Metallicity dependence

The cumulative distribution function of the B[e]SGs and LBVs (including candidates) from this work and the literature. We notice for the first time the presence of B[e]SGs in lower metallicity environments (~0.14 Z_⊙, WLM) and the fact that the two populations are not totally different. We have to be cautious though regarding the low numbers statistics and the completeness issues.



References

- [1] Lamers et al. 1998, A&A, 340, 117
- [2] Humphreys et al. 2014, ApJ, 790, 48
- [3] Ritchie et al. 2009, A&A, 507, 1597
- [4] Kraus 2019, Galaxies, 7, 83,